

Automated analysis of photonic Doppler velocimetry spall signals

Jacob M. Diamond [0000-0001-7905-4260]^{1,2} and K. T. Ramesh [0000-0003-2659-4698]^{1,2*}

¹Department of Mechanical Engineering, Johns Hopkins University, Baltimore, MD, USA.

²Hopkins Extreme Materials Institute (HEMI), Johns Hopkins University, Baltimore, MD, USA.

*Corresponding author(s). E-mail(s): ramesh@jhu.edu;
Contributing authors: jdiamo15@jhu.edu;

Abstract

Recent developments in laser-driven plate impact testing enable hundreds of spall shots per day, with systems being designed that will be capable of thousands of shots per day. Given this volume of data, it is no longer feasible to manually process photonic Doppler velocimetry (PDV) signals for data analyses. In order to match the pace of experimental throughput, we have developed the automated analysis code **AnaLysis of PDV Signals for Spall** (ALPSS). ALPSS is an open-source Python code where the user inputs all necessary parameters within a single function, and the program returns the final velocity trace, spall strength, strain rate, and associated uncertainties, among other quantities. Furthermore, ALPSS is integrated with the Python library watchdog, enabling both real-time analysis of signals during experiments as well as batch processing. Here, we demonstrate ALPSS on a previously analyzed data set, where the fully automated analysis produces only a 2.5% difference in the mean spall strength as compared to manually processed data.

Keywords: PDV, Spall, High-throughput, Automated

1 Introduction and Background

Plate impact experiments are often used to determine the dynamic behavior of materials. Such experiments generate uniaxial strain conditions during early times, and the particle velocity history can be used to infer the stress state in the target as a function of time. The particle velocity is usually measured at the rear surface of the impacted target plate, and the wave propagation characteristics are used to infer states within the target. Such particle velocity measurements are traditionally made using laser interferometric techniques such as VISAR [1], normal displacement interferometry (NDI) [2], or photonic Doppler velocimetry (PDV) [3]. The PDV technique is essentially Michelson interferometry that utilizes fiber optics instead of free space optics [4]. In conventional PDV, light from a stationary reference laser interferes with Doppler-shifted light from another laser (the “target laser”) of the same wavelength that has been reflected off the moving target object. The interference results in a sinusoidal signal that is typically recorded using a digital oscilloscope, with the frequency of the signal containing the information on the motion of the target surface. The out of plane velocity of the target surface is given by [4]

$$v(t) = \frac{\lambda_0}{2} f(t) \quad (1)$$

where λ_0 is the PDV laser wavelength and $f(t)$ is the signal beat frequency, which is generally a function of time. As fiber optic systems and high-bandwidth digital oscilloscopes have become more easily available, the PDV approach has become the technique of choice for many experiments on the dynamic behavior of materials, particularly for high-velocity measurements (10^2 to 10^4 m/s).

In many instances, especially in cases where low velocities are expected, it is common to use “upshifted” PDV. In the upshifted PDV approach, the reference laser beam and the target laser beam have different wavelengths, with the frequency of the target laser being greater than the frequency of the reference laser. This difference in wavelengths generates a beat frequency (called the carrier frequency) even when the target surface is not moving. Calculation of the surface velocity must then also account for this carrier frequency [4, 5]

$$v(t) = \frac{\lambda_T}{2} [f(t) + (f_T - f_R)] \quad (2)$$

where λ_T is the target laser wavelength, $f(t)$ is the signal beat frequency, f_T is the frequency of the target laser, and f_R is the frequency of the reference laser.

Some recent example uses of PDV include equation of state (EOS) measurements [6], Richtmyer-Meshkov instability (RMI) experiments [7], and spall experiments [5]. However, PDV signal processing is not trivial and often requires the time of an experienced user to manually adjust the processing parameters. Several code packages have been created to aid in PDV signal analysis, such as SIRHEN [8], HiFiPDV [9], SAVER [7], and the Sandia TIM finder

[10]. While these packages are well constructed, they all require a significant level of user supervision and guidance.

As high-throughput experimentation becomes more common, there is an increasing need for faster data processing with minimal user intervention. Automated processing using neural networks [11] and short-time auto regression [12] are also being explored. Here we describe an approach to automated analyses of PDV signals that we hope will accelerate the adoption and use of PDV systems for experiments that study the dynamic behavior of materials. We demonstrate the approach through experiments on spall failure conducted within the laser-driven micro-flyer (LDMF) laboratory at Johns Hopkins.

1.1 Spall Failure and Measurements of Spall Strength

For our purposes, we define spallation (or spall failure) as the process of material failure in dynamic uniaxial tensile strain (in metals, this is usually near-hydrostatic tension), with applications ranging from materials characterization to designing protective structures that resist ballistic impact. In plate impact experiments, this state of dynamic tension arises from the interaction of rarefaction fans, which themselves result from the reflection of the initial compressive shock waves from free surfaces. Spallation can be developed during flyer plate impact [13], explosive loading [14], or direct laser drive [15].

In plate impact spall experiments, a “flyer” plate impacts a parallel and stationary target plate, with impact velocities in the range of hundreds to thousands of meters per second. Upon impact, planar compressive shock waves propagate through both the target and the flyer materials. The shock waves reflect from the free surfaces of the target and flyer plates as rarefaction fans which release the compressive state. When the two rarefaction fans meet inside the target, their interaction produces a region of high dynamic tensile stress. If these stresses are sufficiently high, the material of the target plate will fail in tension, typically through the nucleation, growth, and coalescence of voids (and/or cracks). The stress level corresponding to this onset of spall failure is called the spall strength; note that the spall strength depends on the prior compressive shock stress and on the tensile strain rate. This failure creates new free surfaces inside the target, and the signature of this failure process is the corresponding change in the particle velocity at the rear surface of the target plate. A highly idealized velocity profile from a flyer plate spall experiment has the form shown in Fig. 1.

There are several key features that must be extracted from this velocity profile in order to calculate the spall strength and associated tensile strain rate. These features are the points B, C, and D in Fig. 1. From these points, the spall strength, shock stress, and strain rate can be approximated as [5, 16]

$$\sigma_{spall} = \frac{1}{2}\rho C_0(U(t_B) - U(t_D)) \quad (3)$$

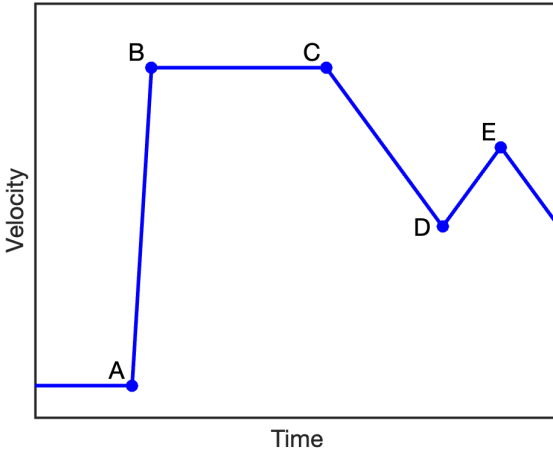


Fig. 1 A highly idealized velocimetry signal from the rear free surface of the target during a flyer plate experiment that involves spall failure.

$$\sigma_{shock} = \frac{1}{2}\rho C_0 U(t_B) \quad (4)$$

$$\dot{\epsilon} = \frac{1}{2C_0} \frac{U(t_C) - U(t_D)}{t_D - t_C} \quad (5)$$

where ρ is the target material density, C_0 is the bulk wave speed in the target material, and U is the particle velocity at any point in time. Additionally, points A and B can be used to find the shock rise time, and points D and E can be used to find the damage growth rate [16]. Such velocity profiles are commonly obtained using interferometric measurements (such as PDV) on the rear free surface of the target, and the velocity profiles are then analyzed as above to determine the spall strength and the dynamic tensile strain rate associated with the spall failure.

Traditional gas-gun-based spall experiments are both expensive and time consuming, with each shot costing thousands of dollars and often taking half a day to run. As a consequence, typical reports in the literature on the spall strength of a material are based on only about 10 shots (thus costing tens of thousands of dollars). However, with recent developments in laser-driven micro-flyer (LDMF) spall testing, we are now capable of running hundreds of shots in a single day [17]. In these LDMF shots, a benchtop 2.5 J Nd:YAG pulsed laser is focused to a 1.67 mm diameter spot to launch a 1.5 mm diameter aluminum flyer of 100 μm thickness. The flyer then impacts a 3 mm diameter target of 200 μm thickness with PDV measuring the back free surface velocity. The rate at which the shots are run is limited mainly by the ability to align the pulsed laser with the next flyer, but shots can be performed every ~60 s with a motorized motion control stage.

Signals from such experiments are of most interest in this paper, but we note that our methods can be used for conventional plate impact experiments as well. A PDV voltage signal and corresponding spectrogram from one of our LDMF spall experiments is shown in Fig. 2, which illustrates the general shape of the spall signals acquired in our experiments, where instead of a traditional square top shock we see a rounded profile with a \sim 10 ns rise time.

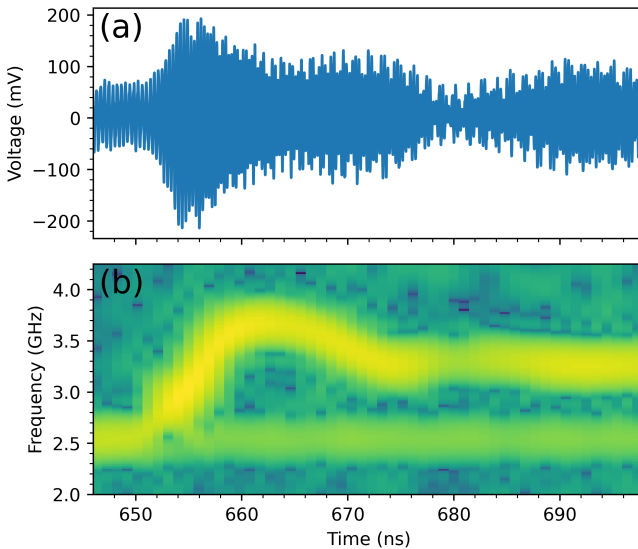


Fig. 2 Representative (a) voltage signal and (b) corresponding spectrogram for a laser-driven micro-flyer (LDMF) spall shot.

Future systems are currently being designed that will enable thousands of shots per day. At this level of experimental throughput, it will be impossible to keep up with the data analysis by manually processing signals one by one. It is necessary to develop a process to rapidly analyze PDV data from spall shots with minimal user intervention. Further, human analysis of such data can provide results that vary based on the analyst, and that also vary from test to test as the human tires from working with a large volume of such data. Here, we present the program **AnaLysis of PDV Signals for Spall** (ALPSS) which is capable of quickly and automatically processing PDV spall signals individually, in real-time during experiments, or via batch processing. We begin by describing the workflow and the structure of the program.

2 Approach to PDV signal analyses

The overall workflow for our PDV analysis protocol is shown in Fig. 3, beginning with the importation of the PDV signal data from the digital oscilloscope. PDV signals are usually worked with as spectrograms [4], and the velocity

history is obtained by analysis of the captured spectrogram. The nature of current PDV signal acquisition is such that much of the acquired spectrogram does not contain useful velocity data, and the first step in PDV signal analysis is to determine the region of interest (ROI) in the spectrogram that contains the appropriate data. Selecting the ROI is traditionally one of the slowest steps in PDV analysis, as most existing programs require the user to manually select or draw the ROI. Once the ROI has been identified, the protocol consists of filtering to isolate the signal, and then the velocity calculation from the signal. At this point, the velocity history has been obtained, and subsequent analysis is determined by the type of experiment performed. For the spall experiments considered here, the next step would be peak finding for the spall analysis, implementation of Eqns. 3, 4, and 5 to obtain the key results, and finally uncertainty analysis. The program is run through a single function containing all necessary parameters, making user adjustments simple and quick. All necessary calculations for the spall strength, strain rate, and associated uncertainties are also built-in, saving the user time during post-processing. We describe each step in some detail within the next few subsections.

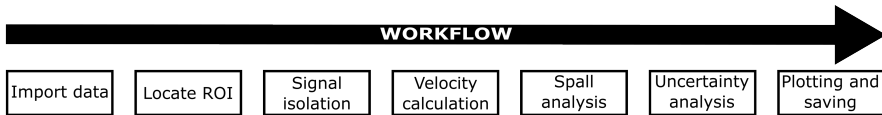


Fig. 3 Overview of the workflow of the PDV spall signal analysis protocol, **AnaLySis of PDV Signals for Spall or ALPSS**.

2.1 Locate the Region of Interest

The first step in the ALPSS program is to identify the region of interest (ROI) where the spall signal is located. This process begins by first importing a user-input range of the original data file (for example, if the original file contains 10 μ s of data, but only 2 μ s are useful, the user has the option to only import the desired 2 μ s time window to reduce computational time). Once the data has been imported, the Short Time Fourier Transform (STFT) [18] is taken to produce a spectrogram of the imported data (Fig. 4a). This spectrogram is then cropped to the user specified frequency range and the powers are logarithmically scaled. Next, using the Python library OpenCV [19], the powers are automatically thresholded using a Gaussian blur filter followed by Otsu's binarization algorithm [20]. In this binarization, spectrogram pixels are broken into two groups, either purple pixels for noise or yellow pixels for the signal (Fig. 4b). Next, the frequency position of the highest yellow pixel is located at each time, denoting the overall top line of the binary signal (Fig. 4b). Then, the average frequency position of the highest yellow pixel for the first 250 ns is taken as the position of the top of the carrier band (Fig. 4b). Lastly, the (global) highest frequency yellow pixel is located and the program

steps backward in time until the top line of yellow pixels in the binary spectrogram intersects the top of the carrier band. The time at which the top of the carrier band is intersected is stored as the start time of the spall signal (Fig. 4b). Otherwise, if the user has input a hard coded value for the signal start time, this process is circumvented altogether, and the signal start time is taken directly as the user input value. Once the signal start time has been found, the program designates the surrounding area as the region of interest (ROI) for the spall signal (Fig 4a).

2.2 Signal Isolation

With the ROI now located, the spall signal must be isolated from the carrier band and noise outside the ROI frequency range. First, the carrier frequency is removed by applying a Gaussian notch filter to the original voltage signal beginning at the signal start time (Fig 4c-d). Afterward, a band pass filter is applied to the voltage signal, where the power of all frequencies outside the ROI are set to zero.

2.3 Calculation of Velocity History

Following isolation, the signal is processed into a velocity trace. Rather than determining the velocity directly from frequencies in the spectrogram, we calculate the velocity as the derivative of the phase angle of the filtered voltage signal, ensuring that the resolution of the velocity trace is equivalent to the sample rate of the oscilloscope [5, 21]. The numerical derivative is calculated using the central difference method with a 9-point stencil. Following differentiation, the velocity trace is smoothed using a Gaussian weighted moving average (Fig. 4e). Note that the analysis process up to this point is useful for any PDV signal, not necessarily only for spall experiments. In the next few subsections, we take this process further forward for the explicit case of spall experiments.

2.4 Spall Analysis

With the smoothed velocity trace now in hand, the program attempts to identify three key points of interest on the spall signal. These points are the global maximum of the signal, the local minimum immediately following the global maximum, and the local maximum immediately following the latter local minimum (Fig. 4f). These points are of interest as they allow for the calculation of the spall strength, peak shock stress, and strain rate (using Eqns. 3, 4, and 5). If all the points are found, the program will automatically calculate all three of these values. If the points cannot be located (e.g. as a result of a poor quality signal or other problems with the shot), they are set to be NaN and the program continues.

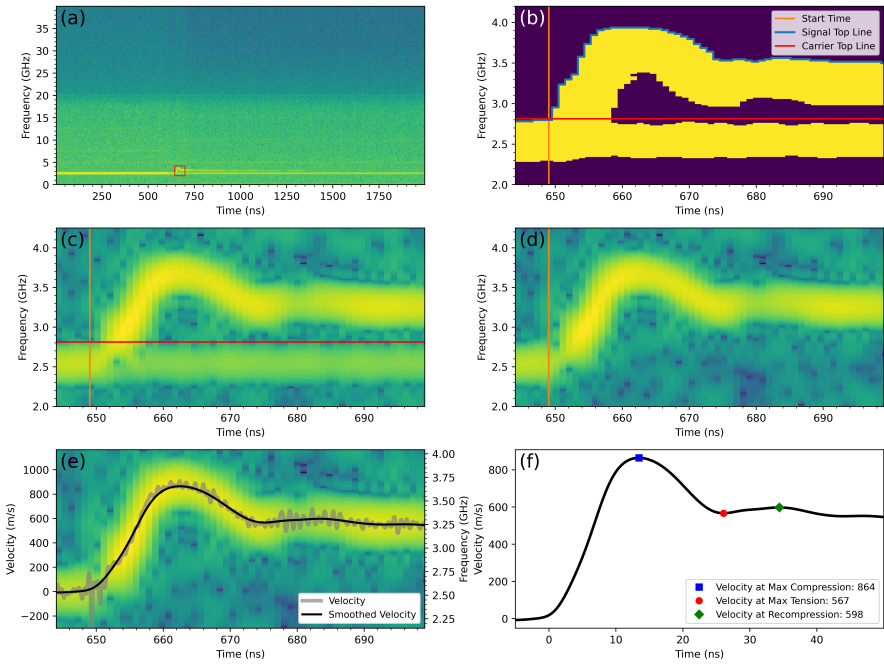


Fig. 4 Sub-processes, (a) spectrogram of imported data with the region of interest (ROI) boxed in red, (b) binary thresholded spectrogram ROI showing the detected locations of the top of the carrier band, the top of the signal, and the signal start time. The signal start time is taken as the point of intersection of the signal top line (blue) and the carrier top line (red), (c) spectrogram ROI with original powers, carrier band location, and signal start time location, (d) spectrogram of the filtered voltage signal, (e) free surface velocity overlaid on the spectrogram, (f) smoothed velocity signal with a re-scaled time axis and the detected velocity points for maximum compression, maximum tension, and recompression.

2.5 Uncertainty Analysis

ALPSS allows the user to calculate the uncertainties associated with the spall strength and strain rate using the equations described by Mallick et al. [5]. These calculations require (one-time only) user inputs as metadata to account for underlying uncertainties in velocimetry and material properties, and return the first-order second moment (first standard deviation) for the spall strength and tensile strain rate.

2.6 Visualization and Saving

If the user chooses, upon the conclusion of the run the analysis code will display a final set of plots and save output files. The final plots show an image for each major step of the analysis process, allowing the user to quickly diagnose the origins of an issue if the program is unsuccessful. Saved outputs consist of a PNG image of the final plots, CSVs of the function inputs used, the velocity trace, the smoothed velocity trace, the filtered voltage signal, and a results file

that includes, the spall strength, strain rate, and uncertainties, among other values that were calculated during the running of the program.

2.7 Error Handling

To prevent the program from crashing while batch processing, the main ALPSS function is wrapped in a *try/except* statement. This is implemented to robustly catch any program failures as an exception, rather than throwing an error and halting the batch process. In the case that the program fails and the *except* statement is reached, ALPSS will output plots of the imported voltage signal and its spectrogram, an error message, and the error traceback. If even that fails, the program will display only the error traceback.

2.8 Real-time analysis during experiments

Incorporation of the *watchdog* library [22] enables real-time analysis during experiments as well as batch processing. One of the benefits of running a large number of high-throughput experiments is the ability to make experimental adjustments during testing. However, this inherently requires the ability to analyze signals quickly after each shot. Watchdog works by monitoring a directory for changes. When it detects that a file has been created (as the voltage signal is saved from the oscilloscope) watchdog automatically calls the ALPSS program and runs the newly created file. This allows the ALPSS code to run without any user intervention, freeing up time to prepare the next shot. Additionally, if the user has already run a series of experiments, the files can be simply dragged to the directory that is being monitored and watchdog will sequentially run all files that have been moved.

2.9 Documentation

Comprehensive documentation for ALPSS is available on GitHub [23]. The documentation covers program installation, details on implementation, and explanations of function inputs, as well as tutorials.

3 Results

To demonstrate the efficacy of the program, we used ALPSS to automatically process PDV signals from 596 real experiments. These experiments were performed over a period of seven months and included different target materials, flyer thicknesses, and flyer velocities [17]. Here, we define a “successful” analysis as an experiment where ALPSS is able to extract the correct spall points without any user intervention or changes to the original input parameters. An “unsuccessful” or “failed” analysis is one in which ALPSS requires changes to the input parameters to automatically extract the correct spall points.

Examining the batch statistics, Fig. 5a shows a one-to-one (1:1) comparison of the spall strengths as determined by ALPSS versus a manual analysis by an experienced human analyst (C. DiMarco in [17]). The results indicate

that the vast majority of spall strengths land on the red 1:1 line, with some landing below the line (meaning ALPSS calculated a lower spall strength than the manual analysis), and a few outliers. The outliers are a result of signals where ALPSS picked different points on the velocity trace versus the user in the manual analysis. This highlights the critical importance of a program that is consistent and unbiased, whereas different human analysts may produce different results for a given signal. In Fig. 5b, the overall spall strength distributions are shown to be nearly identical, with the only difference being a small ($\sim 2.5\%$) difference between the manually processed and the ALPSS mean spall strength values. Lastly, Fig. 5c shows all individual data points for the spall strength versus strain rate. Aside from the outliers where ALPSS selected different spall points from the manual analysis, the individual data points are neatly overlaid except that the ALPSS data points are shifted to both lower spall strengths and lower strain rates. This shift corresponds to the $\sim 2.5\%$ difference in mean spall strength values seen in Fig. 5b, and is likely due to the difference in smoothing procedures used in the different versions of the code for ALPSS and the original manual analysis. ALPSS used a slightly heavier smoothing, which in Fig. 1 would result in points B and C shifting to a lower velocity and point D shifting to a higher velocity. These shifts, according to Eqns. 3 and 5, naturally create an apparent decrease in the spall strength and the strain rate.

ALPSS provides substantial benefits over manual analysis of large data sets. The first benefit is the time savings. The core of the ALPSS program takes only ~ 2 s to run (including all spall strength, strain rate, and uncertainty calculations), with an additional 3 s to 5 s for plotting and saving the results (Apple M1 Pro, 10 cores, 16 GB memory). This processing rate is more than an order of magnitude faster than the 1 min to 2 min it takes to manually process a signal, with the added benefit that the program can run continuously in the background while the user completes other tasks. Results are also repeatable and unbiased, providing a level of consistency that cannot be achieved with existing analysis programs. Since one of the files saved after each run contains the exact input parameters, it is always possible for one user to exactly reconstruct a velocity trace obtained by another user. The automated process never gets tired (experience has shown that the speed of manual analysis depends on the level of fatigue of the human analyst). Lastly, all user parameters are input into a single parent function, making reprocessing with new parameters a trivial task. Even in the case of batch processing hundreds of shots, the user can investigate the effects of different input parameters with the implementation of *watchdog* or a simple *for* loop.

The overall success rate of ALPSS was found to be highly dependent on the signal quality. For batches of experiments with high quality signals and good signal to noise ratios (SNR), success rates reached 80-90%. However, automated analyses of experiments with poor signal quality achieved only $\sim 20\%$ success rates and in practice would require adjustments to input parameters. Even with the wide variability in experimental conditions used to develop the

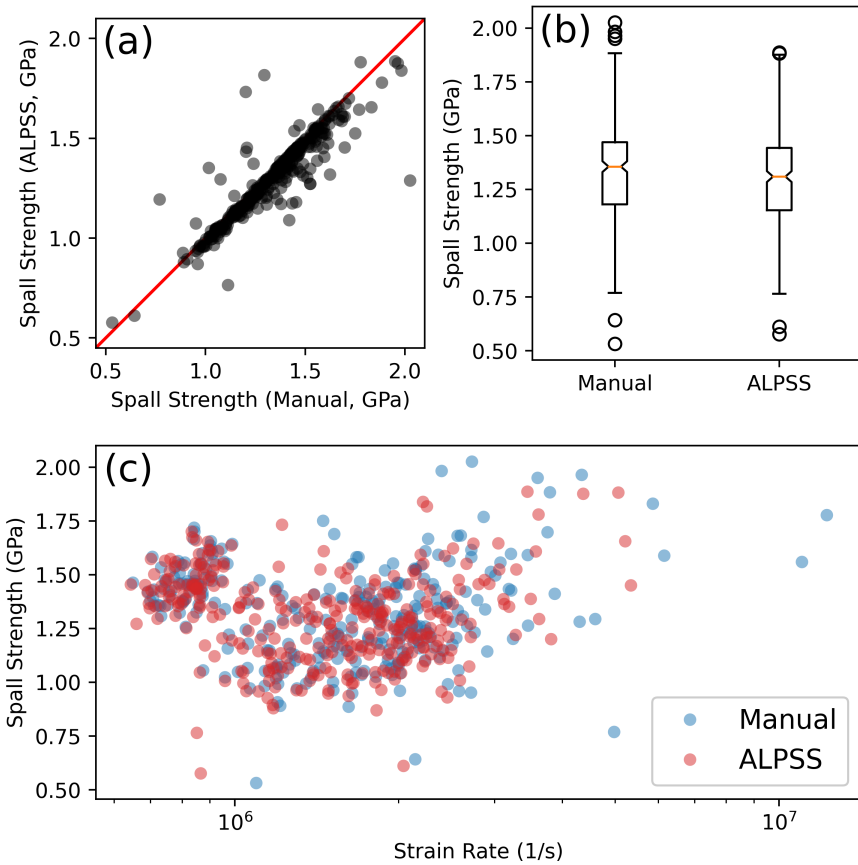


Fig. 5 Comparison to manually processed results with (a) the 1:1 comparison of spall strengths, (b) full distribution of spall strengths, (c) spall strength vs. strain rate.

dataset in this demonstration (including experimental configuration changes within the dataset), the total success rate was 54%, with 323 out of 596 signals successfully processed automatically with no changes required.

There are two cases of experimental signals that have been observed to cause the automated ALPSS process to fail, and which are responsible for the large majority of unsuccessful analyses. These cases stem from poor SNR and (in order of observed frequency) are 1) signal drop-out, and 2) noise around the carrier band. The first case, signal drop-out, represents instances where the SNR drops so low that the original signal information is unresolvable for a certain period of time (Fig. 6a). The second case, noise around the carrier band, often causes the program to choose a signal start time substantially earlier than the true start time (Fig. 6b). In the future, these limitations can be addressed with more advanced signal processing procedures, but that is beyond the current scope of the program.

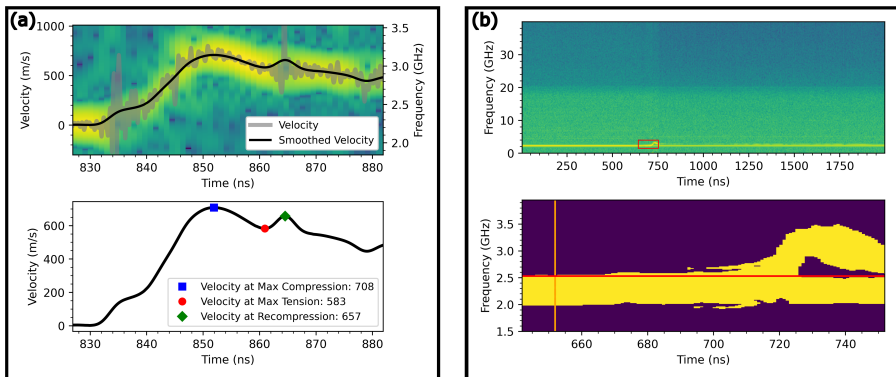


Fig. 6 Representative signals that can cause the automated ALPSS process to fail, (a) signal drop out, where a drop in signal strength causes the velocity to artificially jump. In this case, the signal drops out during pullback (between points C and D in Fig. 1), causing the red max tension and green recompression points to be incorrectly identified. (b) Noise around the carrier band causes the start time of the signal to be incorrectly identified.

These results demonstrate that data from successful automated analyses are trustworthy and closely match manually processed results, while also providing substantial improvements in consistency and processing time. ALPSS currently relies on high quality experimental signals, as poor SNR can drastically reduce the efficacy of the program. Future efforts will be made to introduce more advanced signal processing techniques to mitigate these issues, but in the immediate term it is clear that substantial gains in the success rate can be achieved by improving the quality and consistency of raw experimental signals.

4 Summary

High-throughput characterization of spall strength is a key development that allows us to probe the statistics of a failure phenomenon that can show a great deal of variability depending on loading conditions, material composition, and microstructure. However, experimental throughput has recently been outpacing our capability to process the data. In this work, we introduce the PDV analysis code ALPSS to automatically compute spall strengths from raw PDV signals of laser-driven micro-flyer plate impact experiments. The results shown here demonstrate that ALPSS can reliably and repeatably calculate the spall strength distribution of data, but do so an order of magnitude faster than manual analysis. The program can also calculate uncertainties, run in real-time during experiments, and conduct batch processing. There are two cases of spall signals that can limit the performance of this program (which are discussed earlier in this work) but can be mitigated with improvements to experimental design and future changes to the ALPSS program. ALPSS makes it possible for data analysis to keep up with the pace of high-throughput spall testing, a process that is impossible using existing code packages. This development

allows the field of high-throughput experimentation to advance towards consistently running hundreds or thousands of spall shots per day, without worry of the time it will take to process the data.

Acknowledgements. J.M.D thanks Chris DiMarco, Velat Kilic, Debjoy Mallick, Maggie Eminizer, and David Elbert for their numerous discussions and helpful feedback. Additional thanks to Chris DiMarco for his original hand analysis of the spall data set and to Sam Salander for assistance with programming.

Research was sponsored by the Army Research Laboratory and was accomplished under Cooperative Agreement Number W911NF-22-2-0014. The views and conclusions contained in this document are those of the authors and should not be interpreted as representing the official policies, either expressed or implied, of the Army Research Office or the U.S. Government. The U.S. Government is authorized to reproduce and distribute reprints for Government purposes notwithstanding any copyright notation herein.

CRediT Author Statement. J.M.D: Conceptualization, Software, Investigation, Writing - Original Draft; K.T.R: Supervision, Funding acquisition, Writing - Review & Editing.

Data Availability. The datasets generated during and/or analyzed during the current study are available from the corresponding author upon reasonable request.

Code Availability. All codes and documentation are available on GitHub [23].

Conflict of Interest. All authors declare that they have no conflicts of interest.

References

- [1] Barker, L.M., Hollenbach, R.E.: Laser interferometer for measuring high velocities of any reflecting surface. *Journal of Applied Physics* **43**, 4669–4675 (1972). <https://doi.org/10.1063/1.1660986>
- [2] Clifton, R., Klopp, R.: Pressure-shear plate impact testing. *Metals handbook* **8**(9), 230 (1985)
- [3] Strand, O.T., Berzins, L.V., Goosman, D.R., Kuhlow, W.W., Sargis, P.D., Whitworth, T.L.: Velocimetry using heterodyne techniques, vol. 5580, p. 593. SPIE, ??? (2005). <https://doi.org/10.1117/12.567579>
- [4] Dolan, D.H.: Extreme measurements with photonic doppler velocimetry (pdv). *The Review of scientific instruments* **91**, 051501 (2020). <https://doi.org/10.1063/5.0004363>

- [5] Mallick, D.D., Zhao, M., Parker, J., Kannan, V., Bosworth, B.T., Sagapuram, D., Foster, M.A., Ramesh, K.T.: Laser-driven flyers and nanosecond-resolved velocimetry for spall studies in thin metal foils. *Experimental Mechanics* (2019). <https://doi.org/10.1007/s11340-019-00519-x>
- [6] Jordan, J.L., Casem, D., Zellner, M.: Shock response of polymethyl-methacrylate. *Journal of Dynamic Behavior of Materials* **2**, 372–378 (2016). <https://doi.org/10.1007/s40870-016-0071-5>
- [7] Lear, C.R., Jones, D.R., Prime, M.B., Fensin, S.J.: Saver: A peak velocity extraction program for advanced photonic doppler velocimetry analysis. *Journal of Dynamic Behavior of Materials* **7**, 510–517 (2021). <https://doi.org/10.1007/s40870-021-00295-7>
- [8] Ao, T., Dolan, D.H.: SIRHEN: a Data Reduction Program for Photonic Doppler Velocimetry Measurements. <https://doi.org/10.2172/989357>
- [9] Voorhees, T.J.: High-Precision Measurements and Modeling of How Brittle Granular Materials Behave Under Shock Compression. <http://hdl.handle.net/1853/64148>
- [10] Medina, B.: Determining time of initial motion for upshifted pdv. (2016). <http://hdl.handle.net/1811/78133>
- [11] Frawley, K.G., Sahu, H., Thadhani, N.N., Ramprasad, R.: Predicting velocimetry curves from photonic doppler velocimetry (pdv) signals using neural networks. (2022). <https://doi.org/10.26226/m.62a9d1ee9deaf4fdb6b3fe08>
- [12] Chocron, I., Heim, F., Moore, T., Enriquez-Vargas, R., Barsotti, M., O'Hare, E., Stevens, D.: Laser-driven plate impact technique with application to al6061-t6 hel, spall, and eos. (2022)
- [13] Williams, C.L., Ramesh, K.T., Dandekar, D.P.: Spall response of 1100-o aluminum. *Journal of Applied Physics* **111** (2012). <https://doi.org/10.1063/1.4729305>
- [14] Kanel, G.I., Razorenov, S.V., Bogatch, A., Utkin, A.V., Fortov, V.E., Grady, D.E.: Spall fracture properties of aluminum and magnesium at high temperatures. *Journal of Applied Physics* **79**, 8310–8317 (1996). <https://doi.org/10.1063/1.362542>
- [15] Eliezer, S., Gilath, I., Bar-Noy, T.: Laser-induced spall in metals: Experiment and simulation. *Journal of Applied Physics* **67**, 715–724 (1990). <https://doi.org/10.1063/1.345777>
- [16] Antoun, T., Seaman, L., Curran, D.R., Kanel, G.I., Razorenov, S.V.,

- Utkin, A.V.: Spall Fracture. Springer, ??? (2003)
- [17] DiMarco, C.S., Lim, P., Mallick, D., Kecskes, L., Weihs, T.P., Ramesh, K.T.: Spall failure of ecae mg-al alloys at extreme strain rates: Influence of a refined precipitate and grain microstructure. *Metals* **13**, 454 (2023). <https://doi.org/10.3390/met13030454>
- [18] Virtanen, P., Gommers, R., Oliphant, T.E., Haberland, M., Reddy, T., Cournapeau, D., Burovski, E., Peterson, P., Weckesser, W., Bright, J., van der Walt, S.J., Brett, M., Wilson, J., Millman, K.J., Mayorov, N., Nelson, A.R.J., Jones, E., Kern, R., Larson, E., Carey, C.J., İlhan Polat, Feng, Y., Moore, E.W., VanderPlas, J., Laxalde, D., Perktold, J., Cimrman, R., Henriksen, I., Quintero, E.A., Harris, C.R., Archibald, A.M., Ribeiro, A.H., Pedregosa, F., van Mulbregt, P., Vijaykumar, A., Bardelli, A.P., Rothberg, A., Hilboll, A., Kloeckner, A., Scopatz, A., Lee, A., Rokem, A., Woods, C.N., Fulton, C., Masson, C., Häggström, C., Fitzgerald, C., Nicholson, D.A., Hagen, D.R., Pasechnik, D.V., Olivetti, E., Martin, E., Wieser, E., Silva, F., Lenders, F., Wilhelm, F., Young, G., Price, G.A., Ingold, G.L., Allen, G.E., Lee, G.R., Audren, H., Probst, I., Dietrich, J.P., Silterra, J., Webber, J.T., Slavić, J., Nothman, J., Buchner, J., Kulick, J., Schönberger, J.L., de Miranda Cardoso, J.V., Reimer, J., Harrington, J., Rodríguez, J.L.C., Nunez-Iglesias, J., Kuczynski, J., Tritz, K., Thoma, M., Newville, M., Kümmeler, M., Bolingbroke, M., Tartre, M., Pak, M., Smith, N.J., Nowaczyk, N., Shebanov, N., Pavlyk, O., Brodtkorb, P.A., Lee, P., McGibbon, R.T., Feldbauer, R., Lewis, S., Tygier, S., Sievert, S., Vigna, S., Peterson, S., More, S., Pudlik, T., Oshima, T., Pingel, T.J., Robitaille, T.P., Spura, T., Jones, T.R., Cera, T., Leslie, T., Zito, T., Krauss, T., Upadhyay, U., Halchenko, Y.O., Vázquez-Baeza, Y.: Scipy 1.0: fundamental algorithms for scientific computing in python. *Nature Methods* **17**, 261–272 (2020). <https://doi.org/10.1038/s41592-019-0686-2>
- [19] Bradski, G.: The opencv library. *Dr. Dobb's Journal of Software Tools* **120**, 122–125 (2000)
- [20] Otsu, N.: A threshold selection method from gray-level histograms. *IEEE Transactions on Systems, Man, and Cybernetics* **9**, 62–66 (1979). <https://doi.org/10.1109/TSMC.1979.4310076>
- [21] Mallick, D.D., Zhao, M., Bosworth, B.T., Schuster, B.E., Foster, M.A., Ramesh, K.T.: A simple dual-beam time-multiplexed photon doppler velocimeter for pressure-shear plate impact experiments. *Experimental Mechanics* **59**, 41–49 (2019). <https://doi.org/10.1007/s11340-018-0435-y>
- [22] Mangalapilly, Y.: Watchdog. <https://github.com/gorakhargosh/watchdog>
- [23] Diamond, J.M., Salander, S., Ramesh, K.T.: ALPSS. <https://doi.org/10.>

[5281/zenodo.7603823.](https://zenodo.5281/zenodo.7603823) <https://github.com/Jake-Diamond-9/ALPSS>